Convective-Absolute Transition of non Isothermal Compressible Shear Layer *

ROBINET Jean-Christophe (robinet@paris.ensam.fr)
SINUMEF Laboratory ENSAM-Paris, 151, Boulevard de l'Hopital 75013 Paris, France.

Abstract. The linear stability of inviscid compressible shear layers is studied. When the layer develops at the vicinity of a wall, the two parallel flows can have velocity of the same sign or of opposite sign. This situation is examined in order to obtain first hints on the stability of separated flows in the compressible regime. The shear layer is described by an hyperbolic tangent profile for the velocity component and the Crocco relation for the temperature profile. The gravity effects and the superficial tension are neglected. By examining the temporal growth rate at the saddle point in the wave number space, the flow is characterised as being either absolutely unstable or convectively unstable. This study principally shows the non isothermal effect on the absolute-convective transition in compressible shear flow. Results are presented, showing the amount of the backflow necessary to have this type of transition for a range of primary flow Mach number M_1 up to 3.0. The boundary of the absolute-convective transition is defined as a function of the velocity ratio, the temperature ratio and the Mach number.

Keywords: Convective-absolute transition, shear layer, non isothermal, instability

1. Introduction

An understanding of the stability of compressible shear layers is of fundamental interest and is also important for practical problems found in hypersonic propulsion as the mixing in scramjets and the thrust-vectoring systems. In particular, the shear layer can be regarded as a simple model of the injection device of fuel into an air system. The prediction and the control of such a flow necessitate to know their characteristics and in particular the nature of the instability waves (convective or absolute), which can develop in a shear layer. Linear stability analysis has been used extensively in examining free or confined compressible shear layers. Pioneering work on stability theory of compressible shear flows, both free and wall bounded, is due to (Lee & Lin(1946)), and (Dunn & Lin(1955)) who first showed the importance of three-dimensional disturbances for the stability of these flows. (Lessen *et al.*(1965)), (Blumen *et al.*(1975)), (Tam & Morris(1980)), (Jackson & Grosch(1989); Jackson & Grosch(1990a); Jackson & Grosch(1990b); Jackson & Grosch(1991a); Jackson & Grosch(1991b)) and others have

* The author thanks Pr. J.-P. Dussauge for many helpful comments.

demonstrated that the Kelvin-Helmholtz instability, which was the main instability of the shear layers became less and less amplified as the convective Mach number increased. (Jackson & Grosch(1989)) have shown when the Mach number increased, that the subsonic modes are transformed into supersonic modes which are subsonic at one boundary and supersonic at the other. (Jackson & Grosch(1989)) have shown that there was an infinite set of discrete modes of which the first is a vortical mode and all the others are acoustic modes. They have also shown that three-dimensional disturbances have the same general characteristics as two-dimensional disturbances. On the other hand, a decrease in the temperature ratio $S = T_2/T_1$, where the upper layer quantities are denoted by subscript 1 and the lower ones by subscript 2, results in an increase for the growth rate of the unstable waves at any Mach number. Finally, (Jackson & Grosch(1991a)) have shown that the characteristic features of the solutions to the stability problem for the compressible shear layer are qualitatively similar for a large range of thermodynamic models. Nevertheless, in all these studies, the shear layers were assumed to be free and unconfined. In the case of supersonic shear layers inside a rectangular channel, such as those in a ramjet combustor, see (Tam & Hu(1989)), (Mack(1989)), (Greenough *et al.*(1989)), (Zhuang *et al.*(1989)), (Jackson & Grosch(1990a)) and (Gathmann *et al.*(1993)), the situation is quite different. The unsteady motion of the shear layer is invariably coupled to the acoustic modes of the rectangular channel through reflections of the acoustic waves by the channel walls. (Tam & Hu(1989)) have found that two-dimensional supersonic shear layers inside a rectangular channel may undergo supersonic instabilities. These supersonic instability waves are generated by Mach wave systems formed by reflections from the channel walls. They exist only when the convective Mach numbers of the flow on both sides of the shear layer are supersonic.

Nevertheless, in all of these studies, the type of instability is classified from either its spatial or temporal growth, depending on whether the frequency is real and the wavenumber complex or vice versa. These classifications are quite arbitrary unless one examines carefully the propagative character (i.e., the group velocity) of the instability waves. The work of (Huerre & Monkewitz(1985)) addressed this point and emphasized the important distinction between absolute and convective instability in the context of shear flow. A flow is said absolutely unstable if the response to an impulse in space and time is unbounded everywhere in space for large value of the time. A flow is said to be convectively unstable if the response decays to zero in the reference frame for large time. (Huerre & Monkewitz(1985)) have pointed out that an occurrence of a saddle point in the number wave space may be related to a transition from convective to absolute instability. If such a transition occurs, the spatial stability theory is no longer appropriate and temporal calculations are now required. (Huerre & Monkewitz(1985)) have shown that the incompressible shear layer is convectively unstable for $R = U_2/U_1 > 0$. In fact, they have shown that the shear layer became absolutely unstable only if the low-speed stream had an ambiant speed, say U_2, which was less than $-0.136U_1$, where U_1 is the speed of the high-speed stream. That is, there must be a sufficiently large counterflow before the incompressible shear layer becomes absolutely unstable and a temporal stability theory becomes relevant. The distinction between absolutely or convectively unstable flows, which derives from consideration of the impulse response of the flow, is clearly dependent upon the frame of reference. However, in all laboratory contexts the reference frame is fixed and no ambiguity exists. Furthermore, these concepts become particularly significant in non-parallel flows where the propagative character of the instability may change locally as the flow develops in the streamwise direction and, consequently, another intrinsic length scale (the streamwise length scale over which the flow is absolutely unstable) should be introduced, which can have an important dynamical role in determining the response of the flow. In some particular conditions, this can lead to a strong frequency selection mechanism and force a long-range spatial order to the flow. The absolute-convective classification of an instability is also an important issue in regard to flow control. Localized forcing of a flow in order to influence its space-time development will be effective, perhaps, only if the flow is convectively unstable. In an absolutely unstable flow the forcing will be rapidly overwhelmed by the in situ growing instability. For this reason, it is useful to define the parameter ranges wherein a flow is either absolutely or convectively unstable. Nevertheless, the absolute-convective transition in the shear layer in a three-dimensional compressible fluid has not been studied as extensively as in an incompressible fluid. Independently, (Pavithran & Redekopp(1989)) and (Jackson & Grosch(1990b)) have studied the transition from convective to absolute instability in a compressible, subsonic two-dimensional, free shear layer. They found that as the Mach number increased in the subsonic regime, so did the amount of backflow necessary to go from convective to absolute instability. They also found that when the slow stream was cooled with respect to the high-speed stream at a fixed Mach number, the amount of backflow necessary to go from convective to absolute instability decreased. However, their studies are limited to the subsonic regime and for two-dimensional waves. To our knowledge, there is not studies dealing with the convective-absolute transition of a free shear layer in supersonic regime. Only (Peroomian & Kelly(1994)) have studied the convective-absolute transition in a compressible supersonic flow, but in confined shear layers with constant mean temperature, density and pressure and for two-dimensional waves. They found that in the subsonic case, $M_1 < 1$, only one α_+ mode exists, and the calculation of the transition boundary is straightforward. However, in the supersonic case multiple modes exist, and extreme care must be taken in the evaluation of the saddle point. This is due to the fact that when multiple modes exist in a system, coalescence can occur between two α_+ modes as well as α_+ and α_- modes. For $1 < M_1 < 1.32$, initially the subsonic/subsonic mode becomes absolutely unstable. However, if the backflow parameter is sufficiently increased, the subsonic/supersonic modes becomes the primary pinched mode, i.e., pinching for this mode occurs at a lower positive value of ω_{0_i}. At $M_1 = 1.32$, this change occurs at $\omega_{0_i} = 0$ and for $1.32 < M_1 < 1.35$ this change in the pinching of the modes occurs for a negative value of ω_{0_i}. For Mach numbers greater than 1.35, the primary mode is the subsonic/supersonic mode, and remains so up to the point near $M_1 \simeq 1.9$, where the mode becomes a supersonic/supersonic mode. Nevertheless, in their analysis, the three-dimensional and the temperature effects have not been taken into acount on the convective-absolute transition.

In the present paper, we will examine the inviscid convective-absolute transition of a two-dimensional compressible free and confined shear layer with a particular attention to the non isothermal effect on this convective-absolute transition. In §2 we give the general assumptions, the mathematical form of the perturbation and the mean flow. In §3 we formulate the stability problem and the boundary conditions. In §4, the numerical method used is briefly presented. Section 5 contains a presentation of our numerical results, in particular the convective-absolute transition from a supersonic confined or not confined, isothermal or not isothermal shear layer disturbed by 2D fluctuations is analyzed. Conclusions are given in §6.

2. General assumptions, mathematical form of the perturbation and mean flow

The general equations of motion for the instantaneous flow are the Euler equations, the energy equation, written for the total energy and the equation of state for a perfect gas. The boundary condition imposed in the present problem expresses that there is no variation of fluctuations far from the shear layer and that viscosity is not considered on the walls $\pm y_w$ (where y_w is the wall distance).

The present stability theory is based on the classical small perturbations technique where the instantaneous flow is the superposition of the known mean flow and unknown fluctuations. All the physical quantities q (velocity, pressure,$\cdots$) are decomposed into a mean value and a fluctuating one:

$$q(x, y, z, t) = \bar{q}(y) + q_f(x, y, z, t), \tag{1}$$

where the mean flow is supposed to be parallel, i.e. it only depends on the y direction.

We consider a two-dimensional compressible shear layer, with zero pressure gradient, which separates two streams of different speeds and temperatures. We assume that the mean flow is governed by the compressible boundary layer equations. The x-axis is taken along the direction of the flow, the y-axis normal to the flow. Let ($\bar{U}$,$\bar{V}$,0) be the velocity components in (x, y, z) directions, respectively, $\bar{\rho}$ the density and $\bar{T}$ the temperature of this mean flow. All variables are non-dimensionalized using upper layer values at $y \to \infty$ or $y = +y_w$. The structure of the mean flow clearly depends on the variation of the viscosity coefficient $\bar{\mu}$ and the Prandtl number P_r with the temperature and pressure. In general, both $\bar{\mu}$ and P_r are very weakly dependent on pressure and can be taken to be independent of pressure. The Prandtl number is somewhat dependent on the temperature but, in this study it will be assumed to be constant. Finally, the dependence of viscosity on temperature is quite important and can be related to different thermodynamic models, see (Jackson & Grosch(1991a)). However as indicated in the introduction, the various thermodynamic models give qualitatively similar results for a spatial stability analysis. As pressure is constant and the state equation is written in canonical from $\bar{\rho}\bar{T} = 1$. When, the viscosity is supposed to be proportional to the temperature, that is we use the Chapman viscosity law, $\bar{\mu}(\bar{T}) = C\bar{T}$ and that $P_r = 1$, the solution of the mean flow equations has a similarity solution given by (Lock(1951)). However, as discussed in (Jackson & Grosch(1991a)), the qualitative stability characteristics are independent of the detailed shape of the mean profile. For this reason we use the Crocco relation, with the boundary conditions

$$\begin{gathered}\bar{U} \to 1,\, \bar{T} \to 1 \quad \text{as} \quad \eta \to +\eta_w, \quad \bar{U} \to R,\, \bar{T} \to S \quad \text{as} \quad \eta \to -\eta_w, \\ \eta_w \to \infty \quad \text{for the free shear layer.}\end{gathered} \tag{2}$$

The temperature and velocity profiles are thus written as

$$\bar{T}(\eta) = S\frac{1-\bar{U}}{1-R} + \frac{\bar{U}-R}{1-R} + \frac{1}{2}(\gamma-1)\bar{M}_1^2(\bar{U}-R)(1-\bar{U}) \quad (3)$$

and

$$\bar{U}(\eta) = \frac{1}{2}\left[1+R+(1-R)\tanh(\eta)\right], \quad (4)$$

where $\bar{U}$ is an good approximation of the Lock profile. γ is the ratio of specific heats, and $\bar{M}_1$ is the Mach number defined as the ratio of the speed of the upper stream to the speed of sound. R and S are respectively the ratio of streamwise velocity and of temperature between the lower flow and the upper flow. The parameter range of interest for the velocity ratio is $-1 < R < 1$ and $S > 0$ for the temperature ratio. When $-1 < R < 0$, the low-speed stream is opposed to the high-speed stream and when $R > 0$ the two streams are coflowing. If S is less than one, the lower stream is colder than the upper stream and if S is greater than one, the lower flow is warmer. Figure 1 shows the corresponding velocity and temperature profiles. The shear layer thickness is defined

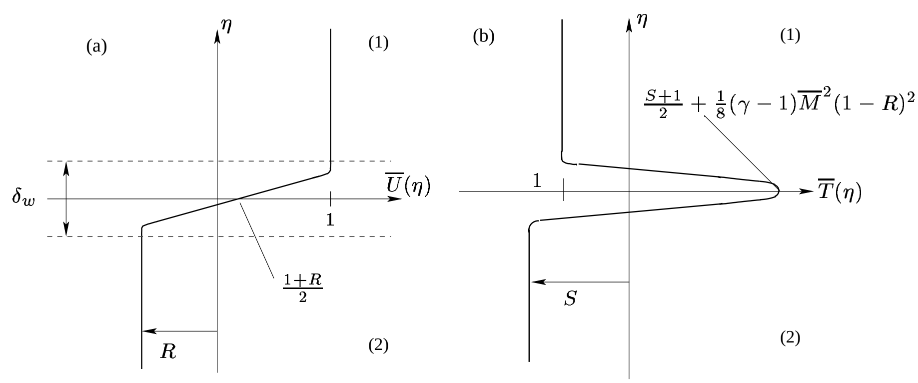

Figure 1. Sketch of different characteristics of the mean flow, (a) velocity profile, (b) temperature profile.

as: $\delta_w = (1-R)/\max(d\bar{U}/d\eta)$. In this case, δ_w is equal to 2.

3. Stability problem and general theoretical results

3.1. Linearised Euler equations

The basic flow is perturbed by introducing wave disturbances for the velocity, pressure, temperature and density with amplitudes which are functions of y only. According to the homogeneous form of the boundary conditions as well as the y-dependence of the mean flow (parallel assumption), the perturbation can be described as a normal mode with respect to x, z, t variables. Any perturbation (pressure, velocity, temperature,...) can be written in the normal mode form

$$\underline{Z}_f(x, \eta, z, t) = \underline{\tilde{Z}}(\eta) e^{i(\alpha x + \beta z - \omega t)}, \tag{5}$$

where $\underline{\tilde{Z}} = \left(\tilde{p}, \tilde{u}, \tilde{v}, \tilde{w}, \tilde{T}\right)^t$ is the function amplitude vector of the fluctuation, $\underline{k} = (\alpha, \beta)^t$ is a wave number vector with α and β the wave numbers in the downstream (x) and cross-stream (z) directions, respectively and ω the circular frequency. In the general stability context, β is real, ω and α are *a priori* complex and their real parts are the magnitude of the frequency and the wave number respectively, while their imaginary parts indicate whether the disturbance is amplified, neutral, or damped depending on whether ω_i and $-\alpha_i$ are negative, zero or positive. In the following β is supposed to be equal to zero. The decomposition (1) with the perturbation form (5) is introduced into instantaneous governing equations. The resulting equations are then simplified by taking into account, firstly that the mean quantities satisfy the equations and secondly that the fluctuating quantities are assumed to be small, so that the equations can be linearized with respect to the disturbance. Finally, the linearized Euler equations lead to the well-known compressible Rayleigh equation written for the pressure.

$$\left\{ \frac{d^2}{d\eta^2} - \frac{2}{\bar{U} - c} \frac{d\bar{U}}{d\eta} \frac{d}{d\eta} - \alpha^2 \bar{T} \left[\bar{T} - M^2 \left(\bar{U} - c \right)^2 \right] \right\} \tilde{p}(\eta) = 0. \tag{6}$$

Here, c is the complex phase wave velocity $c = \omega / \alpha$. The equation (6) is solved with the following boundary conditions:

$$\lim_{\eta \to \pm \eta_w} \frac{d\tilde{p}}{d\eta} = 0, \;\; \eta_w \to \infty \text{ for free shear layer.} \tag{7}$$

For a given control parameter (R, S), equation (6) with the boundary condition (7) form a linear eigenvalue problem for the parallel shear flow since a non-zero solution $\tilde{p}$ exists if and only if the complex set (α, ω) fulfills a relation $\mathcal{D}(\alpha, \omega; R, S) = 0$.

The purpose here is to define the propagative character of the unstable disturbances, i.e. to know if the basic flow is absolutely or convectively unstable, it is thus necessary to solve (6) and (7) along with the condition of zero group velocity

$$\mathcal{D}(\alpha_0, \omega_0; R, S) = 0 \text{ and } \frac{\partial \mathcal{D}}{\partial \alpha}(\alpha_0, \omega_0; R, S) = 0 \tag{8}$$

and, in particular, the identification of these values (α_0, ω_0) corresponding to zeros of $\partial\omega/\partial\alpha$. The value ω_0 is, therefore, a square-root branch point of the function $\alpha(\omega)$ and the point α_0 in the complex α-plane corresponds to a saddle point formed by the intersection of upstream spatial branch $\alpha_+(\omega)$ and downstream spatial branch $\alpha_-(\omega)$. The nature of the instability is determined by the location of the branch point in the complex ω-plane. The instability is of absolute type if the branch point is in the upper-half-plane ($\omega_i > 0$) and is of convective type if it is in lower-half-plane ($\omega_i < 0$). Hence, the transition occurs for parameters values (i.e., R, S, $\bar{M}$) for which the branch point lies on the real ω-axis. This is essentially the Briggs-Bers criterion, see also (Huerre & Monkewitz(1985)).

4. Numerical resolutions

As clearly highlighted by (Malik(1985); Malik(1990)), the spectral collocation method based on Chebyshev polynomials provides an accurate and powerful tool when numerically solving the eigenvalue problem. The implementation of a spectral algorithm based upon collocation is almost as straightforward as the finite-difference scheme once the derivative matrices are set up. The use of collocation also simplifies the treatment of boundary conditions and coordinate transformations. In recent years, multi-domain spectral methods have become fashionable for fluid mechanics problems. The method is described here for two domains. The physical domain $-\eta_w \leq \eta \leq \eta_w$ is divided into two domains $-\eta_w \leq \eta \leq \eta_i$ and $\eta_i \leq \eta \leq \eta_w$ which may be denoted as domain I and domain II, respectively. In the present paper, η_i is the altitude of the generalized inflection point $d(\bar{T}^{-2} d\bar{U}/d\eta)/d\eta|_{\eta_i} = 0$. Note that this expression differs from that given by (Lee & Lin(1946)) by a factor $\bar{T}^{-1}$ because they wrote this expression in term of y and we have chosen, like (Jackson & Grosch(1989)), to write it in term of η. The stability equation (6) now may be written in the two domains as

$$D_I^2\tilde{p}_I + A_I D_I \tilde{p}_I + B_I \tilde{p}_I = 0 \text{ and } D_{II}^2\tilde{p}_{II} + A_{II} D_{II}\tilde{p}_{II} + B_{II}\tilde{p}_{II} = 0,$$
$$\text{with } D_I = D_{II} \equiv \tfrac{d}{d\eta},$$

and with the boundary conditions:

$$D_I\tilde{p}_I = 0 \text{ as } \eta \to -\eta_w \text{ and } D_{II}\tilde{p}_{II} = 0 \text{ as } \eta \to +\eta_w.$$

In addition, we need interface conditions at $\eta = \eta_i$. These are provided by requiring the derivability of $\tilde{p}$ at $\eta = \eta_i$, i.e., $D_I\tilde{p}_I(\eta_i) = D_{II}\tilde{p}_{II}(\eta_i)$. The physical domains $-\eta_w \le \eta \le \eta_i$ and $\eta_i \le \eta \le +\eta_w$ are now transformed to the computational domains. We use Nth order Chebyshev polynomials T_N defined in the interval $-1 \le \xi_j^i \le 1$, $i = I$ or II, where the collocation points ξ_j^i are the extrema of T_n and are given by

$$\xi_j^i = \cos\frac{\pi j}{N_i},\ \ j = 0, \cdots, N_i,\ \ i = I \text{ or } II. \tag{9}$$

Chebyshev collocation method is applied separately to the two domains with collocation points. In order to apply the spectral collocation method, an interpolant polynomial is constructed for the dependent variables in terms of their values at the collocation points. Thus an Nth order polynomial may be written as

$$\tilde{p}_i(\xi^i) = \sum_{k=0}^{N_i} a_k^i(\xi^i)\tilde{p}_i(\xi_k),\ \ i = I \text{ or } II, \tag{10}$$

where the interpolant $a_k^i(\xi^i)$ for the Chebyshev scheme is given by

$$a_k^i(\xi^i) = \left(\tfrac{1-\xi_k^2}{\xi^i-\xi_k}\right)\tfrac{T_N'(\xi^i)}{N^2 c_k}(-1)^{k+1},$$
$$\text{where } c_0 = c_N = 2,\ c_k = 1, \text{ for } k \in \{1,..,N-1\}, \text{ and } i = I \text{ or } II.$$

The first derivative of $\tilde{p}_i(\xi^i)$ may be written as

$$\left.\frac{d\tilde{p}_i}{d\xi^i}\right|_j = \sum_{k=0}^{N_i} E_{jk}^i \tilde{p}_{i,k},\ \ i = I \text{ or } II, \tag{11}$$

where E_{jk}^i are the elements of the derivative matrix given by

$$E_{jk}^i = \tfrac{c_j}{c_k}\tfrac{(-1)^{k+j}}{\xi_j^i-\xi_k^i};\ j \ne k,\ \ E_{jj}^i = -\tfrac{\xi_j^i}{2(1-{\xi_j^i}^2)},$$
$$E_{00}^i = \tfrac{2N_i^2+1}{6} = -E_{N_iN_i}^i,\ \ i = I \text{ or } II.$$

The scaling factor for the transformation between physical and computational domains is given as $S_j^i = \partial\xi^i/\partial\eta\ |_j;\ j = 0, \cdots, N_i$, then the first derivative matrix F in the physical domain may be written as

$$F_{jk}^i = S_j^i E_{jk}^i, \tag{12}$$

and the second derivative matrix G^i_{jk} is simply $G^i_{jk} = F^i_{jm}F^i_{mk}$. Now the stability equation (6) may be written at the collocation points ξ^i_j as

$$\sum_{k=0}^{N_i} G^i_{jk}\tilde{p}_{i,k} + A^i_j \sum_{k=0}^{N_i} F^i_{jk}\tilde{p}_{i,k} + B^i_j\tilde{p}_{i,k} = 0, \;\; i = I \text{ or } II. \qquad (13)$$

Finally, Eqs (13) with the boundary conditions $D_i\tilde{p}_i(\pm y_w) = 0$ may be represented as

$$\begin{gathered}\left(\underline{\underline{C_3}}\alpha^3 + \underline{\underline{C_2}}\alpha^2 + \underline{\underline{C_1}}\alpha + \underline{\underline{C_0}}\right)\underline{\phi} = 0,\\ \text{with } \underline{\phi} = (\tilde{p}_0, \cdots, \tilde{p}_N)^t \text{ where } N = N_1 + N_2.\end{gathered} \qquad (14)$$

(14) represents the discretized eigenvalue problem.
The Chebyshev interval $-1 \leq \xi \leq 1$ is transformed to the computational domain $-\eta_w \leq \eta \leq \eta_w$ by use of the mapping

$$\eta_I = -\frac{\eta_w}{2}(\xi_I + 1)\,,\; \eta_{II} = \frac{\eta_w}{2}(1 - \xi_{II})$$

for the confined shear layer and for the free shear layer ($\eta_w \to \infty$) the mapping

$$\eta_{(I,II)} = a\frac{\xi_{(I,II)} + 1}{b - \xi_{(I,II)}}, \text{ with } a = \frac{\eta_a\eta_w}{(\eta_w - 2\eta_a)} \text{ and } b = 1 + \frac{2a}{\eta_w}.$$

In your case $\eta_a \simeq \delta_w$, where δ_w is the shear layer thickness. A standard eigenvalue subroutine may now be used to compute the $N+1$ eigenvalues. Two methods were used to solve the equation (14): a local method based on a shooting method with a classical Newton-Raphson algorithm and a global method, where the discretized operator spectrum is computed, see (Bridges & Morris(1984)). In the results presented below, the number of points in each domain is respectively: $N_1 = 100$ and $N_2 = 200$ for the free shear layer and $N_1 = 100$ and $N_2 = 100$ for the confined shear layer.

To determine the convective-absolute transition, the saddle point for the present system is found by three different numerical techniques. The first method involves the calculation of the branches $\alpha^+(\omega)$ and $\alpha^-(\omega)$ corresponding to $x > 0$ and $x < 0$, respectively, for different ω until pinching is observed. The second is a Taylor series fit near the saddle point, which is a square root branch point in the complex wave number plane. The third is a direct numerical method using Newton-Raphson's technique for solving $\partial\omega/\partial\alpha = 0$. However, this last method is hightly dependent on the initial guess provided for the saddle point location, and once the solution converges, it cannot be said without *a priori* knowledge if the converged solution is the location of coalescence of two α^+ modes or of an α^+ mode and an α^- mode. In this study, the first method is systematically used with the second method. Occasionally, the third method is employed as a check of our results.

5. Results

In the present section, the case of convective-absolute transition in free and confined shear layers is studied. Results are presented, and in particular the amount of backflow necessary to have this type of transition for a range of primary flow Mach number, $\bar{M}_1$ up to 3.0. The boundary of the absolute-convective transition is defined as a function of the velocitity ratio R, the temperature ratio S and the Mach number $\bar{M}_1$.

5.1. Free shear layer

5.1.1. *Two-dimensional instability wave and isothermal flow*

Two sets of results have been obtained, which are presented here. First, the variation of the velocity ratio and stability parameters with Mach number $\bar{M}_1$ under the requirement that the square-root branch point of $\alpha(\omega)$ lies on the real ω-axis (convective-absolute transition) for isothermal ($S = 1$) flow is shown. Second, the variation of these same parameters with temperature ratio S for prescribed Mach number $\bar{M}_1$, requiring again that the branch point is located on the real ω-axis is also shown. The pertinent stability parameters in each case are the real branch point frequency ω_{0_r} and the real and the imaginary parts of the wave-number (α_{0_r}, α_{0_i}) of the corresponding saddle point in the α-plane. Fig. 2 gives the parametric variation of the critical branch point location separating the domains of absolute and convective instabilities in the $(R, \bar{M}_1)$ plane for isothermal shear layer. The intercept value of R at $\bar{M}_1 = 0$ coincides with the value -0.136 computed by (Huerre & Monkewitz(1985)). Figure 2.a shows that the shear flow remains convectively unstable with increasing backflow on the low-speed side as the Mach number increases. This trend remains true for $\bar{M}_1 \leq 1.448$. In fact, for this Mach number range, the phase speed of the instability wave is subsonic. Our results differ from those of (Pavithran & Redekopp(1989)) by at most 10% because their temperature profile is not given by the Crocco relation. Instead, their temperature equation is equivalent to that obtained from (3) by dropping the Mach squared term. (Jackson & Grosch(1990b)) have obtained similar results, who, unlike (Pavithran & Redekopp(1989)), did not neglect the

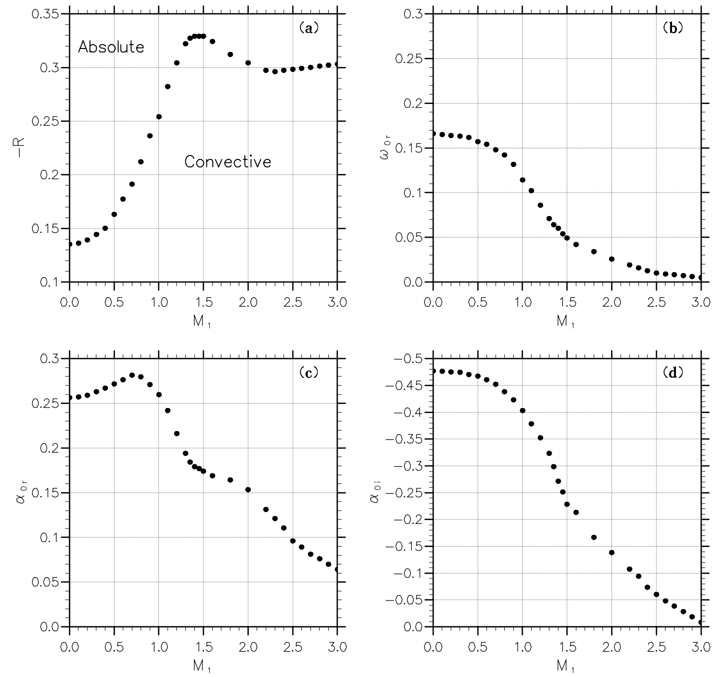

Figure 2. The absolute-convective transition boundary (a) and variation of the branch point parameters with high-speed side Mach number $\bar{M}_1$: (b) circular frequency ω_0; (c) wave number α_{0_r}; (d) the spatial growth rate α_{0_i} for two-dimensional disturbance ($\theta = 0^o$) and isothermal shear layer ($S = 1$).

Mach number square term in the temperature profile. However in their analysis, the convective-absolute transition is limited to the subsonic isothermal shear layer with a two-dimensional disturbance ($\theta = 0^o$). Our results are within 2% of their results. In our knowledge, the study of the convective-absolute transition for a supersonic shear layer was not carried out. When the Mach number is greater than 1.448, the phase speed of the instability wave becomes supersonic at $+\infty$ and subsonic at $-\infty$, the evolution of the absolute-convective transition boundary changes in this regime. When the phase speed of the instability wave becomes supersonic, the boundary of the convective-absolute transition continues to increase until $\bar{M}_1 \simeq 1.5$ ($-R \simeq 0.33$) and it stabilizes around $R = -0.3$ when $\bar{M}_1 > 2.1$. The variation of the branch point parameters with the Mach number is given in figure 2.b,c,d. The trends are monotonic with the Mach number, except for the real part of the wavenumber. The decrease of α_{0_i}, as $\bar{M}_1$ tends to unity, may be associated with the stabilization of the continuation of the Kelvin-Helmholtz instability in incompressible flow and the decreasing bandwidth of unstable wavenumbers α_r for this mode. The branch point frequency decreases substantially for Mach numbers above 0.3, where compressibility effects become significant. For these branch point parameters the modification of the instability wave nature can be seen from a slope change in their evolutions with respect to Mach number. When the Mach number increases, the absolute frequency ω_0 (figure 2.b) and the absolute spatial growth rate α_{0_i} (figure 2.d) tend towards to zero. For a high Mach number ($\bar{M}_1 \geq 3$) the convective-absolute transition looses its significance because the absolute spatial growth rate is close to zero. However, it should be remembered that additional modes of instabiliy are present for $\bar{M}_1$ greater than unity. Indeed, the works of (Jackson & Grosch(1989)) and (Mack(1989)) have shown, for a purely spatial instability, that there are supersonic modes. However, for $\bar{M}_1 \leq 3$ these modes are not dominant in the convective-absolute transition for free shear layer (no pinching have been observed). Figure

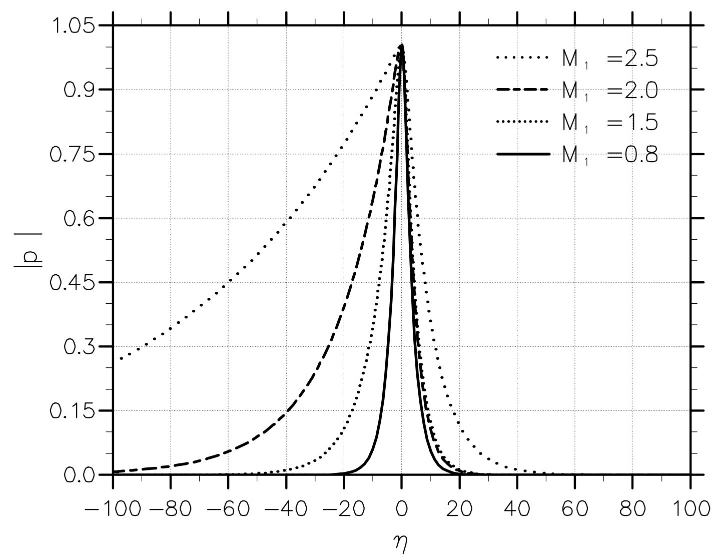

Figure 3. Eigenfunctions (pressure amplitude) for different Mach numbers $\bar{M}_1 = 0.8$, 1.5, 2.0 2.5, for $S = 1$, $\theta = 0^o$ and with $\pm\eta_w = 300$.

3 shows typical pressure eigenfunction instability waves for several Mach numbers. As the Mach number increases, the decrease of the pressure fluctuation on the low speed side is increasingly weak. This characteristics is representative of the supersonic phase speed of the instability wave.

5.1.2. *Two-dimensional instability wave and non isothermal flow*

The influence of the temperature ratio S on the absolute-convective transition boundary is shown in Fig. 4. It is clear that the temperature

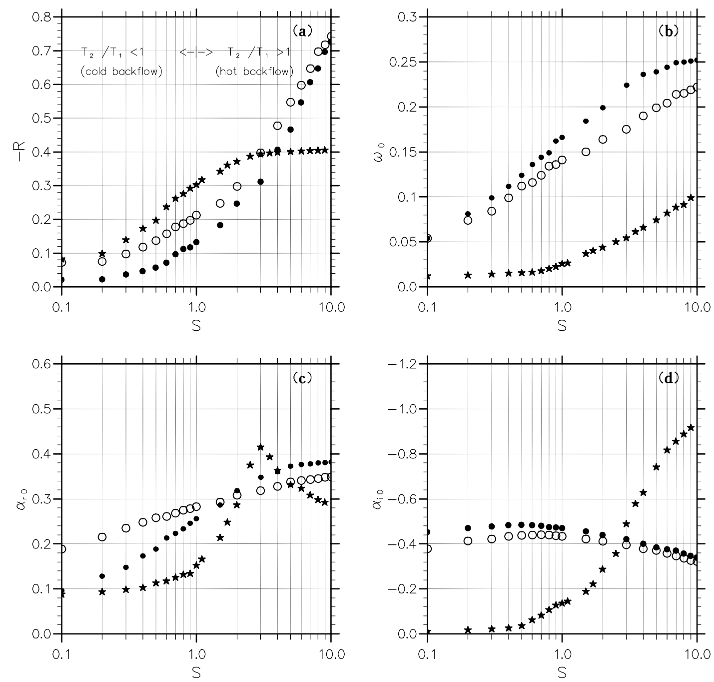

Figure 4. The absolute-convective transition boundary (a) and variation of the branch point parameters versus $S = \bar{T}_2/\bar{T}_1$: (b) circular frequency ω_0; (c) wave number α_{0_r}; (d) the spatial growth rate α_{0_i} for different Mach numbers: $\bar{M}_1 = 0$ ($\bullet$), 0.8 ($\circ$), 2.0 ($\star$) and for a two-dimensional perturbation ($\theta = 0^o$).

ratio has a larger influence than the Mach number on the transition velocity ratio over the entire range. It is observed that cooling the low-speed side can causes a convectively unstable shear layer at fixed velocity ratio to become absolutely unstable. When $S < 1$, only a small amount of backflow is required on the low-speed side ($\bar{U}_2 = -0.0745\bar{U}_1$, for a subsonic compressible flow ($\bar{M}_1 = 0.8$)). These results are consistent with the calculations presented by (Pavithran & Redekopp(1989)). The transition velocity ratio for $\bar{M}_1 = 0.8$ was calculated for $S = 0.1$ and $S = 10$, we have obtained $R = -0.0745$ and $R = -0.745$, respectively. These values are within about one percent of those reported by (Pavithran & Redekopp(1989)) ($R = -0.074$ and $R = -0.74$, when they used the temperature profile obtained by Crocco's relation). The variation of the branch point parameters with the temperature ratio for a subsonic Mach number ($\bar{M}_1 = 0$ and 0.8) are close to those obtained by (Pavithran & Redekopp(1989)) and (Jackson & Grosch(1989)). These evolutions are presented in figures 4.b,c,d. In supersonic regime, the evolution of the branch point parameters can be qualitatively different. When the temperature ratio

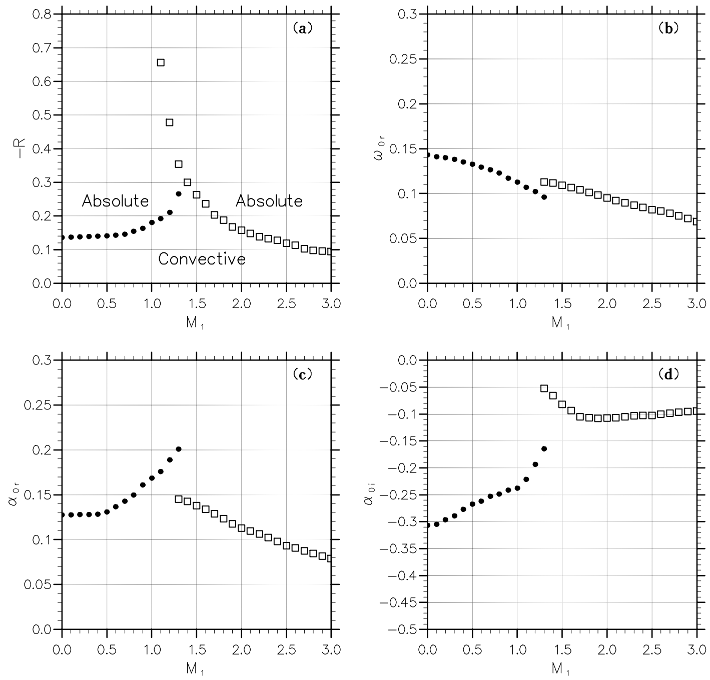

Figure 5. The absolute-convective transition boundary (a) and variation of the branch point parameters with upper-layer Mach number $\bar{M}_1$: (b) circular frequency ω_0; (c) wave number α_{0_r}; (d) the spatial growth rate α_{0_i} for two-dimensional disturbance ($\theta = 0^o$) and isothermal shear layer ($S = 1$), (•): mode 1, (□): mode 2.

changes, the nature of the instability also changes. For example, if $\bar{M}_1 = 2$ and if $S < 0.4$ then the phase speed of the instability wave is supersonic/supersonic. On the other hand if $0.4 \leq S \leq 3.225$ the phase speed is subsonic/supersonic. Finally, if $S > 3.225$ the phase speed is always subsonic/supersonic but with $\bar{M}_1 < \bar{M}^*$. In this last case, the evolution of the absolute wavenumber (α_{0_r} and α_{0_i}) is qualitatively different (see Fig. 4.c and 4.d).

5.2. Confined shear layer

5.2.1. *Two-dimensional instability wave and isothermal flow*

In this section, the local two-dimensional stability characteristics of a confined compressible shear layer are studied. The mean flow is defined as in the previous section, the mean velocity profile is modelled as a finite length shear layer with a hyperbolic tangent velocity profile (4) and the mean temperature profile is given by Crocco's relation (3). The wall are localised, in a first step, at $\eta = \pm\eta_w$ with $\eta_w = 10$. At this distance, the mean flow is uniform. These boundary conditions are identical to those chosen by (Peroomian & Kelly(1994)). However, in their case, the mean temperature, density and pressure have been chosen constant and the instability wave was sought two-dimensional. Figure 5.a shows the backflow necessary for transition between convective and absolute instability for different values of the Mach number $\bar{M}_1$. The subsonic portion of Fig. 5.a qualitatively agrees (about 2%) with the work of (Pavithran & Redekopp(1989)) and of (Jackson & Grosch(1989)). The amount of backflow necessary for transition from convective to absolute instability increases as the Mach number increases. In the subsonic case, the wall effect does not influence the transition convective-absolute. However, the branch point parameters (ω_0, α_0) are affected. For a confined subsonic shear layer, the absolute frequency is close to that obtained for a free shear layer, but this is not the case for the absolute wavenumber. In the confined case, the absolute wavelength is almost twice larger, and the absolute growth rate is 1.6 weaker than in the case of the free shear layer (see Fig. 2). For the subsonic case, $\bar{M}_1 < 1.0$, only one α_+ mode exists, but in the supersonic case multiple modes exist, and extreme care must be taken in the evaluation of the saddle point. This is due to the fact that when multiple modes exist in the system, coalescence can occur between two α_+ branches as well as a α_+ and α_- branch. In Fig. 5.a, once the mean flow becomes supersonic, the characteristics of the transition boundary change. The absolutely unstable mode for the subsonic Mach numbers remains the dominant mode when $1.0 < \bar{M}_1 < 1.32$ (dominant in the sense that it becomes absolutely unstable for the smallest $-R$ value). The associated phase speed with this mode is subsonic/subsonic (called mode 1). However another mode exists but it is not dominant for this Mach number range, this mode is subsonic/supersonic. Indeed, if one increases the backflow parameter sufficiently, the subsonic/supersonic mode (called mode 2) becomes the primary mode, i.e., pinching for this mode occurs at a lower positive value of ω_{0_i}. At $\bar{M}_1 = 1.32$, where the cusp in the curve is located (see Fig. 5), this change occurs at $\omega_{0_i} = 0$. For $1.32 < \bar{M}_1 < 1.345$, this change in the pinching of the modes occurs for a negative ω_{0_i}. Figure 6 shows the evolution of the imaginary part of the absolute frequency ω_{0_i} for different Mach numbers. In the case $\bar{M}_1 = 1.25$, the first mode becomes absolutely unstable when $-R > 0.22$ and it becomes again unstable convectively when $-R > 0.47$. For this Mach number, the second mode becomes absolutely unstable for $-R > 0.42$. For $\bar{M}_1 = 1.32$, the transition from convective to absolute (CA), for mode 1, occurs when $-R = 0.26$ and the reverse transition, from absolute to convective (AC), occurs when $-R = 0.35$. For the second mode, the transition CA occurs when $-R = 0.356$. In fact, for $1.32 < \bar{M}_1 < 1.345$ a small region exists

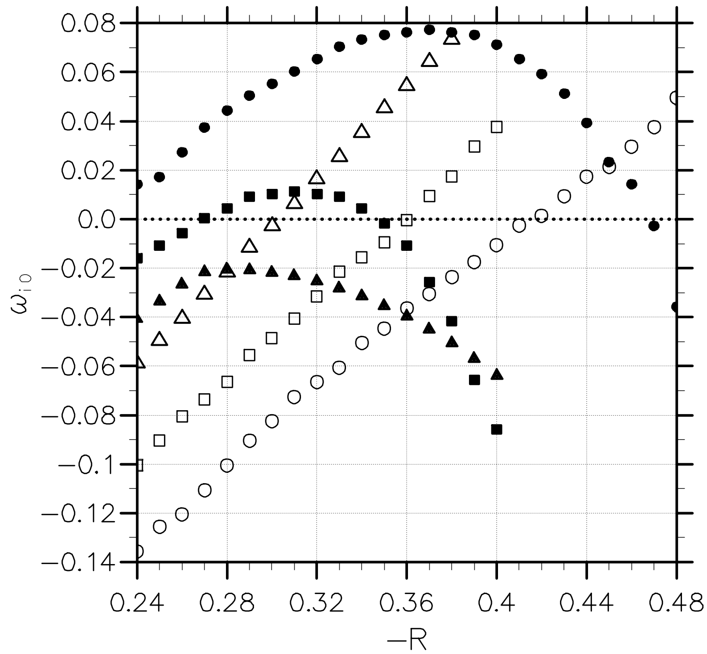

Figure 6. Imaginary part of saddle point frequency versus the backflow parameter R for different Mach number: $\bar{M}_1 = 1.25$, • (mode 1), ∘ (mode 2); $\bar{M}_1 = 1.32$, ■ (mode 1), □ (mode 2); $\bar{M}_1 = 1.4$, ▲ (mode 1), △ (mode 2).

between $0.35 < -R < 0.356$ where the two modes are convectively unstable. This corresponds to the region in Fig. 5.a, where the boundary has turned back on itself near the cusp. It is however highly possible that this particular characteristic is modified by the nonparallel or the non linear effects. Beyond this Mach number, $\bar{M}_1 = 1.345$, mode 1 is not absolutely unstable, only mode 2 becomes absolutely unstable. Figure 6 shows this characteristic for $\bar{M}_1 = 1.4$. For Mach numbers greater then 1.345, the primary mode is the subsonic/supersonic mode, and remains so up to the point near $\bar{M}_1 \simeq 1.95$, where the mode becomes a supersonic/supersonic mode. This mode selection, which is dependent on R, was already observed by (Peroomian & Kelly(1994)), but they had not taken into account the mean temperature profile, which is clearly nonconstant for these Mach number ranges. However, our results are close to those obtained by (Peroomian & Kelly(1994)) (within between 1% and 5%). For the temperature profile given by Crocco's relation, the CA transition occurs for a lower value of the backflow than in the case where the temperature profile is constant.

Physically, in the linear stability context, this shows that in the region between $1.32 < \bar{M}_1 < 1.345$, as the backflow parameter increased, the

Table I. Wall effects on the CA transition for mode 2: $\bar{M}_1 = 1.32$, $S = 1$ and $\theta = 0$.

$\mid \eta_w \mid$	R	ω_0	α_0
07	-0.387	0.1660	0.208-0.093i
08	-0.380	0.1450	0.184-0.076i
09	-0.372	0.1288	0.168-0.064i
10	-0.356	0.1135	0.146-0.059i
11	-0.353	0.1043	0.135-0.044i
12	-0.350	0.0953	0.126-0.034i
14	-0.348	0.0807	0.108-0.023i
17	-0.346	0.0757	0.088-0.015i
20	-0.340	0.0551	0.072-0.0089i
>24, the CA transition does not exist.			

flow becomes absolutely unstable. If the backflow is further increased, the mode becomes convectively unstable once again, and a further increase in backflow will make a different mode absolutely unstable. This is due to the fact that multiple modes exist when $\bar{M}_1 > 1$. When the backflow parameter is increased for a fixed $\bar{M}_1$, the shear is increased and the spatial growth rate for the subsonic/subsonic mode decreases; the spatial growth rate for the subsonic/supersonic increases, this causes the subsonic/supersonic mode to eventually become the primary pinched mode. However, further increase in the backflow causes a jump in the branch point parameters. Indeed, this occurs for the same R, S, $\bar{M}_1$ and ω_{0_i} but for a different ω_{0_r}, α_{0_r} and α_{0_i}.
Table I shows the wall influence on the transition CA for mode 2. When $\mid \eta_w \mid$ increases, the backflow required to achieve the transition CA decreases but the absolute spatial growth rate also decreases until becoming neutral, at this distance, $\mid \eta_w \mid \simeq 24$, the transition CA does not exist. For a supersonic shear layer, the existence of a wall plays a determining role in the characterization of instabilities. Figure 7 shows typical eigenfunction (pressure) distributions of subsonic/supersonic instability waves (mode 2) and subsonic/subsonic instability waves (mode 1).

5.2.2. *Two-dimensional instability wave and non isothermal flow*
The influence of the temperature ratio (S) on the convective-absolute transition boundary is shown in Figs. 8.a to 8.d. Again in this case, it is clear that the temperature ratio has a large influence on CA transition.

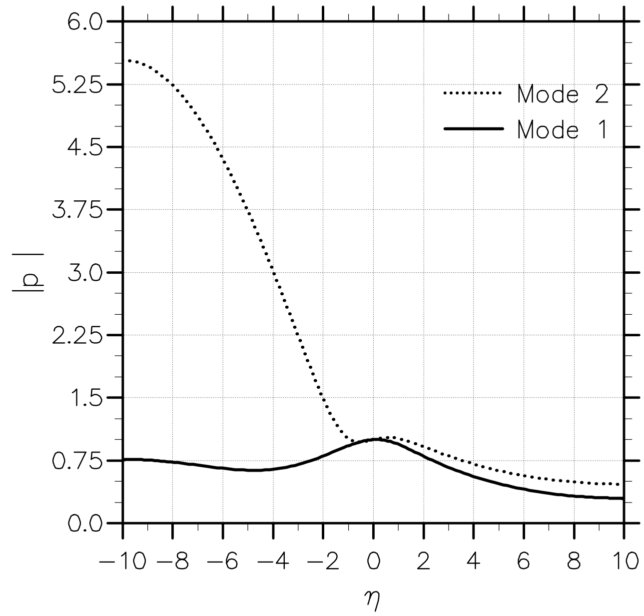

Figure 7. Eigenfunctions (pressure amplitude) for the mode 1 and 2, for $\bar{M}_1 = 1.31$, $S = 1$, $\theta = 0^o$ and with $\pm\eta_w = 10$.

As for the free shear flow, it is observed that the cooling of the low-speed side can cause a convectively unstable shear layer at fixed velocity ratio to become absolutely unstable. This effect seems to be true for a large Mach number range ($0 < \bar{M}_1 < 3.0$). However, there exists a significant difference in the influence of S on the CA transition for a free shear layer and for a confined shear layer. This can be found in the evolution of α_0 when instability wave has, at least, its phase speed supersonic in one of shear layer side. Figures 4.c, 4.d, 8.c and 8.d show these differences.

6. Conclusions

A detailed analysis of the convective-absolute nature of the instability of two-dimensional supersonic shear layer has been made. When the Mach number $\bar{M}_1 < 1$, for a given velocity ratio, the shear layer becomes more convectively unstable as the Mach number increases. This trend persists, for fixed Mach number, as the low-speed side is heated relative to the high-speed side. On the other land, cooling the low-speed side extends the domain of absolute instability. In fact, for sufficiently small temperature ratio (viz, $S < 0.1$), the shear layer may become absolutely unstable, even when the streams are a very weak

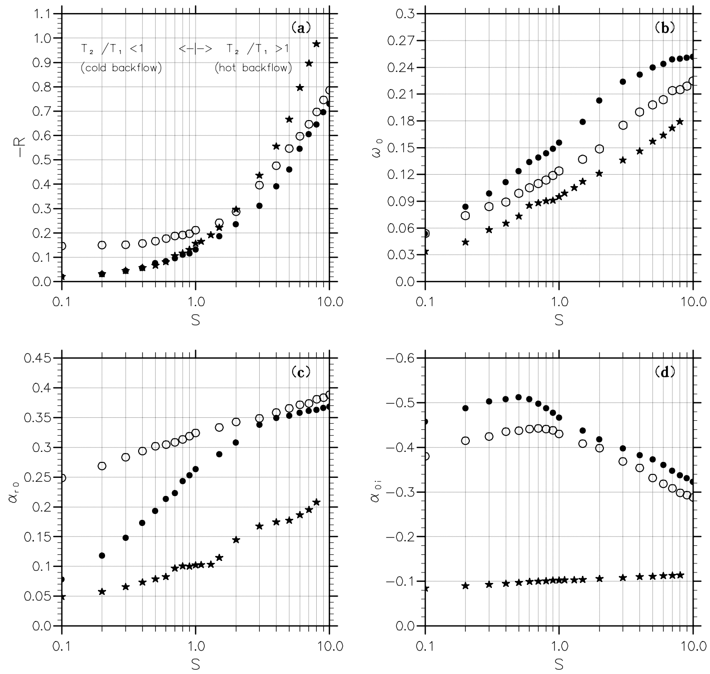

Figure 8. The absolute-convective transition boundary (a) and variation of the branch point parameters versus $S = \bar{T}_2/\bar{T}_1$: (b) circular frequency ω_0; (c) wave number α_{r_0}; (d) the spatial growth rate α_{i_0} for different Mach numbers: $\bar{M}_1 = 0$ ($\bullet$), 0.8 ($\circ$), 2.0 ($\star$) and for two-dimensional perturbation ($\theta = 0^o$).

counterflowing. In the subsonic regime, the most unstable instability wave is two-dimensional and the boundary between convective and absolute instability is thus determined by the pinching between 2 two-dimensional subsonic/subsonic modes. The effect of the parallel walls and the distance between them on the instability characteristics of the shear flow were investigated. The distance between such walls does not affect qualitatively the characteristics of the CA transition.

However, when the Mach number is supersonic, the effects of the walls have a large importance in the CA transition. When the distance is decreased the reflections of the compression/expansion waves caused by the walls provide a feedback mechanism between the growing shear layer structure and the wave system. Moreover, when $\bar{M}_1 > 1$, multiple modes exist and the coalescence can occur between two α_+ modes as well as between α_+ and α_- modes.
When the walls are far enough ($\delta_w \ll \eta_w$), the boundary of the CA transition is determined by the pinching of the extension of the modes in the subsonic regime. According to Mach number $\bar{M}_1$ and the temperature

ratio S, this pinching mode is subsonic/subsonic, subsonic/supersonic or supersonic/supersonic. In all these cases, the characteristics of the branch point parameters $(\omega_0,\, \alpha_0)$ are quite different. When the walls are close to the shear layer, the transition curve for $\bar{M}_1$ between 0 and 1.0 and between 1.345 and 3.0 is defined by a single curve. However for $\bar{M}_1$ between 1.0 and 1.345, multiple transition curves exist, due to the fact that multiple modes exist when $\bar{M}_1$ is greater than unity. In this region, the mode that becomes absolutely unstable depends on the magnitude of the backflow. For a non isothermal (free or confined) shear flow, the conclusions are identical with those presented for $\bar{M}_1 < 1$, the only evolution of the branch point parameters being highly dependant on η_w.

These results have particular relevance to the issue of control of shear layers since injected disturbances can modify the streamwise evolution of a convectively unstable flow. Moreover, this analysis is a preliminary study for the characterisation of the convective-absolute transition in separated supersonic boundary layer. As a separated boundary layer behaves like as shear layer with a counterflow and with a wall on the low-speed side, the knowledge of the CA transition in such shear layers is a useful guide to evaluate the CA transition in separated boundary layer. Indeed, we have shown so that a supersonic shear layer can develop an absolute instability, it is necessary either to cool the lower side of the shear layer or that $-R > 0.3$. In realistic supersonic separated boundary layer, the intensity of the backflow does not exceed 15% of the external flow. It seems reasonable to think that the instabilities developing in a separated supersonic boundary layer are linearly convectively unstable. Finally, this analysis can undoubtedly apply in the industrial case of a wall cooled by a cold cooling film, for example for the hot nozzle flow.

References

Lee, L. & Lin, C. C. (1946). Investigation of the stability of the laminar boundary layer in a compressible fluid. NACA TN 1115.

Dunn, D. W. & Lin, C. C. (1955). On the stability of the laminar bounary in a compressible fluid. J. Aero. Sci. 22, 455-477.

Lessen, L., Fox, J. A. & Zien. H. M. (1965). On the stability of the laminar mixing of two parallel streams of a compressible fluid. J. Fluid Mech. 23. 355-367.

Lessen, L., Fox, J. A. & Zien. H. M. (1966). Stability of the laminar mixing of two parallel streams with respect to supersonic disturbances. J. Fluid Mech. 25. 737-742.

Blumen, W., Drazin, P. G. & Billings, D. F. (1975). Shear layer instability of an inviscid compressible fluid. Part 2. J. Fluid Mech. 71, 305-316.

Tam, C. K. W., & Morris, P. J. (1980). The radiation of sound by the instability waves of a compressible plane turbulent shear layer. J. Fluid Mech. 98, 349-381.

Jackson, T. L., & Grosch C. E. (1989). Inviscid spatial stability of a compressible mixing layer. J. Fluid Mech. 208, 609-637.

Jackson, T. L., & Grosch C. E. (1990). Inviscid spatial stability of a compressible mixing layer. Part 2. The flame sheet model. J. Fluid Mech. 217, 391-420.

Jackson, T. L., & Grosch C. E. (1991). Inviscid spatial stability of a compressible mixing layer. Part 3. Effect of thermodynamics. J. Fluid Mech. 224, 159-175.

Jackson, T. L., & Grosch C. E. (1991). Inviscid spatial stability of a three-dimensional compressible mixing layer. J. Fluid Mech. 231, 35-50.

Tam, C. K. W., & Hu, F. Q. (1989). The instability and acoustic wave modes of supersonic mixing layers inside a rectangular channel. J. Fluid Mech. 203, 51-76.

Mack, L. (1989). On the inviscid acoustic-mode instability of supersonic shear flows. Fourth Symposium on Numerical and Physical Aspects of Aerodynamics Flows, pp. 1-15. California State University, Long Beach, CA.

Gathmann, R. J., Si-Ameur, M. & Mathey F. (1993). Numerical simulation of three-dimensional natural transition in the compressible confined shear layer. Phys. Fluids A 5(11), 2946-2968.

Greenough, J. A., Riley, J. J., Soestrino M. and Eberhardt D. S. (1989). The effects of walls on a compresible mixing layer. AIAA Paper 89-0372.

Zhuang, M., Dimotakis, P. E. & Kubota T. (1989). The effect of walls on a spatially growing supersonic shear layer. Phys. Fluids A 2(4), 599-604.

Bridges T. J., & Morris P. J. (1984). Differential Eigenvalue Problems in Which the parameter Appears Nonlinearly. Journal of Computational Physics. 55, 437-460.

Huerre, P., & Monkewitz, P. (1985). Absolute and convective instabilities in free shear layers. J. Fluid Mech. 159, 151-168.

Pavithran, S., & Redekopp, L. G. (1989). The absolute-convective transition in subsonic mixing layers. Phys. Fluids. A. 1(10), 1736-1739.

Jackson, T. L., & Grosch C. E. (1990). Absolute/convective instabilites and the convective Mach number in a compressible mixing layer. Phys. Fluids A. 2(6), 949-955.

Peroomian, O., & Kelly R. E. (1994). Absolute and convective instabilites in a compressible confined mixing layer. Phys. Fluids. 6(9), 3192-3194.

Lock., R. C. (1951). The velocity distribution in the laminar boundary layer between parallel streams. Q. J. Mech. Appl. Maths. 4, 42-63.

Malik. M. R., Zang. T. A. & Hussaini M. Y. (1985). A spectral Collocation Method for the Navier-Stokes Equations. Journal of Computational Physics. 61, 64-88.

Malik., M. R. (1990). Numerical Methods for Hypersonic Boundary Layer Stability. Journal of Computational Physics. 86, 376-413.

Briggs., R. J. (1964). Electron-Stream Interaction with Plasmas. (MIT Press, Cambridge Mass).